AMERICAN ACADEMY OF OPHTHALMOLOGY®

Topical Nanoemulsion of a Runt-related Transcription Factor 1 Inhibitor for the Treatment of Pathologic Ocular Angiogenesis

Santiago Delgado-Tirado, MD,[1,2,*] Lucia Gonzalez-Buendia, MD,[1,2,3,*] Miranda An, BA,[1,2] Dhanesh Amarnani, MS,[1,2] Daniela Isaacs-Bernal, BSc,[1,2] Hannah Whitmore, PhD,[1,2] Said Arevalo-Alquichire, PhD,[1,2,4] David Leyton-Cifuentes, BME,[1,2,5] Jose M. Ruiz-Moreno, MD, PhD,[3,6] Joseph F. Arboleda-Velasquez, MD, PhD,[1,2,7] Leo A. Kim, MD, PhD[1,2]

Purpose: To test the efficacy of runt-related transcription factor 1 (RUNX1) inhibition with topical nanoemulsion containing Ro5-3335 (eNano-Ro5) in experimental ocular neovascularization.

Design: Preclinical experimental study.

Participants: In vitro primary culture human retinal endothelial cell (HREC) culture. C57BL/6J 6- to 10-week-old male and female mice.

Methods: We evaluated the effect of eNano-Ro5 in cell proliferation, cell toxicity, and migration of HRECs. We used an alkali burn model of corneal neovascularization and a laser-induced model of choroidal neovascularization to test in vivo efficacy of eNano-Ro5 in pathologic angiogenesis in mice. We used mass spectrometry to measure penetration of Ro5-3335 released from the nanoemulsion in ocular tissues.

Main Outcome Measures: Neovascular area.

Results: RUNX1 inhibition reduced cell proliferation and migration in vitro. Mass spectrometry analysis revealed detectable levels of the active RUNX1 small-molecule inhibitor Ro5-3335 in the anterior and posterior segment of the mice eyes. Topical treatment with eNano-Ro5 significantly reduced corneal neovascularization and improved corneal wound healing after alkali burn. Choroidal neovascularization lesion size and leakage were significantly reduced after treatment with topical eNano-Ro5.

Conclusions: Topical treatment with eNano-Ro5 is an effective and viable platform to deliver a small-molecule RUNX1 inhibitor. This route of administration offers advantages that could improve the management and outcomes of these sight-threatening conditions. Topical noninvasive delivery of RUNX1 inhibitor could be beneficial for many patients with pathologic ocular neovascularization. *Ophthalmology Science 2022;2:100163* © *2022 by the American Academy of Ophthalmology. This is an open access article under the CC BY-NC-ND license (http://creativecommons.org/licenses/by-nc-nd/4.0/).*

Supplemental material available at www.ophthalmologyscience.org.

Ocular neovascularization is a hallmark of multiple ophthalmic diseases, including exudative age-related macular degeneration (AMD), proliferative diabetic retinopathy, hemorrhagic glaucoma, and corneal neovascularization. Ocular neovascularization is characterized by aberrant angiogenesis and vascular leakage and proliferation, leading to edema and hemorrhages. Common complications include corneal opacification, glaucoma, and retinal detachment. All these events, if untreated, can lead to irreversible vision loss.[1,2]

Neovascularization is tightly regulated by multiple growth factors, including VEGF.[3] Management of neovascular ocular diseases has changed significantly in the last decade with the approval of anti-VEGF therapies.[3,4] Intravitreal administration of anti-VEGF drugs has allowed a remarkable improvement in the natural course of ocular diseases such as neovascular AMD and proliferative diabetic retinopathy.[4,5]

Despite the success of anti-VEGF treatments, they are not completely efficacious or free of side effects. These therapies have been associated with the onset of hemorrhages and worsening of tractional retinal detachment in patients with diabetic retinopathy and of atrophy in patients with AMD.[6–9] This is of particular importance in the clinic, because 98.2% of patients with neovascular AMD demonstrate areas of atrophy in the macula,[10] impacting not only the visual acuity of these patients, but also their quality of life. Incomplete response to anti-VEGF therapy has been reported in almost 50% of patients with neovascular

https://doi.org/10.1016/j.xops.2022.100163
ISSN 2666-9145/22

AMD.[11] Diseases affecting the cornea are a common cause of vision loss, and the presence of new abnormal blood vessels invading the corneal tissue is frequently seen in these patients.[12] The prevalence of corneal neovascularization in the United States is estimated to be approximately 4.14%, affecting 1.4 million people per year,[12] and to date no clear guidelines exist for the management of this condition.

Recently, our group identified a transcription factor called runt-related transcription factor 1 (RUNX1) as a major modulator of retinal and choroidal aberrant angiogenesis.[13,14] The small-molecule RUNX1 inhibitor, Ro5-3335, administered intravitreally, significantly reduced the development of aberrant retinal angiogenesis in a model of oxygen-induced retinopathy.[13] Also, intravitreal injections of Ro5-3335, in monotherapy or in combination with anti-VEGF, reduced vascular leakage and lesion size in a laser-induced choroidal neovascularization model.[14] Mechanistic studies unambiguously demonstrated that RUNX1 operates as a proangiogenic pathway alternate to VEGF.[15]

We surmise that topical administration of an RUNX1 inhibitor may be a practical approach to address ocular conditions. In a proof-of-concept experiment, topical application of Ro5-3335 nanoemulsion (eNano-Ro5) reduced progression of proliferative vitreoretinopathy in a rabbit model.[16] This analysis was justified by our discovery of a critical role for RUNX1 in the pathobiological characteristics of aberrant epithelial-to-mesenchymal transition (EMT), a process leading to the formation of fibrotic membranes within the eye, often as a complication of ocular trauma or retinal detachment in proliferative vitreoretinopathy. These data support the idea that RUNX1 function is critical to processes regulating EMT and aberrant angiogenesis. Importantly, fibrosis also occurs in vitreoretinal membranes resulting from AMD and proliferative diabetic retinopathy, triggering retinal traction and tears. This phenomenon, the angiofibrotic switch, is not alleviated, and in some cases worsens, with anti-VEGF therapies.[17] Therefore, the therapeutic effect of a topical eNano-Ro5 nanoemulsion was studied.

Methods

eNano-Ro5 Preparation Procedure

eNano-Ro5 was obtained following a previously published protocol.[16] In brief, the oil phase of the mixture was prepared using lecithin and isopropyl myristate (172472; Millipore Sigma) in a 1:1 proportion. Next, 10 mg of RUNX1 inhibitor (Ro5-3335; 219506 [Millipore Sigma]) was added to the oil phase. Sterile phosphate-buffered saline (PBS) was added as the aqueous phase to the mixture to form a single phase with a final concentration of 7.92 mM. Finally, pretreatment with homogenization and subsequent sonication was carried out to obtain the nanoemulsion system (Fig 1A).

In Vitro Experiments

Cell Culture. For all in vitro experiments, human retinal endothelial cells (HRECs; Cell Systems) were incubated at 37°C in 5% carbon dioxide using standard endothelial growth media (Lonza) supplemented with 2% fetal bovine serum (Atlanta Biologicals), 1% penicillin plus streptomycin, and 1% L-glutamine (Lonza).

Cell Proliferation and Cytotoxicity Assays. Human retinal endothelial cells were cultured to reach 90% confluency per well and were treated with different concentrations of eNano-Ro5 mixed with HREC media (0.5%, 1%, and 2%) or nanoemulsion without Ro5-3335 (vehicle) as a control. After 24 hours, supernatant was obtained and lactate dehydrogenase levels were measured to analyze cytotoxicity using the Cytotoxicity Assay kit (Promega). Proliferation was evaluated 48 hours after the treatment media was added. Cells were washed and fixed (4% paraformaldehyde for 10 minutes) before permeabilization (0.5% Triton X-100 in PBS for 5 minutes) and blocking (10% goat serum in PBS for 1 hour at room temperature). To assess proliferation, cells were incubated with anti-Ki67 antibody (1:50; Novus Biologicals) in antibody dilution buffer (5% goat serum) and incubated overnight at 4°C. Cells were incubated with secondary antibody goat antirabbit Alexa Fluor 594 (Life Technologies) at 1:300 dilution for 2 hours at room temperature. Cells were washed in PBS and stained using Prolong Gold Antifade Reagent with 4',6-diamidino-2-phenylindole (DAPI). Images were obtained using an EVOS FL Auto imaging system (Life Technologies). The quantification is reported as an average of Ki67-positive cells to the number of DAPI-positive cells per high-powered field of HREC culture, which were cultured in triplicate.

Scratch-Wound Migration Assay. Human retinal endothelial cell migratory capacity was assessed by scratch-wound assay. Cells were cultured until a confluent monolayer was obtained. Then, using a 200-μl pipette tip, a scratch was generated to induce cell migration as described.[18] For this evaluation, only 2% of the eNano-Ro5 group was assessed because this concentration showed best results in cell proliferation analysis. Nanoemulsion without Ro5-3335 (vehicle) was used as a control group. Images were obtained 0, 6, 12, 24, 48, 72, and 96 hours after scratch using an EVOS FL automated stage live cell imaging system. All the experiments were performed in triplicate, and migration was measured as the wound closure rate related to time 0 using the TScratch Matlab module.

In Vivo Experiments

The Institutional Animal Care Committee of Massachusetts Eye and Ear reviewed and approved all animal procedures performed in this study. All experiments were carried out in accordance with the Association for Research in Vision and Ophthalmology Statement for the Use of Animals in Ophthalmic and Vision Research.

C57BL/6J male and female mice 6 to 10 weeks of age purchased from Jackson Laboratories were used. Before every procedure, mice were anesthetized by intraperitoneal injection of ketamine plus xylazine mixture (100/50 mg/kg; KetaVed [Vedco, Inc] and Anased [Akorn Animal Health]). Pupils were dilated by topical application of 1% tropicamide drops (Bausch & Lomb, Inc), and local anesthesia was obtained by instillation of 0.5% proparacaine (Bausch & Lomb, Inc). Genteal gel (Alcon) was applied as an optical contact and lubricant. Animals were maintained in a temperature-controlled, 12-hour day−night cycle environment with food and water ad libitum. Samples were collected after euthanasia in carbon dioxide chamber. Animal Research: Reporting of In Vivo Experiments (ARRIVE) guidelines were followed for the report of the information regarding in vivo experiments in this article.[19]

Mice Alkali Burn Model. A 2-mm paper disc soaked in 1 M NaOH was placed directly on the surface of the central cornea for 30 seconds, followed by thorough washing with saline solution for 60 seconds. To avoid dripping liquid, the filter paper disc was tapped on an absorbable pad before placing it over the central

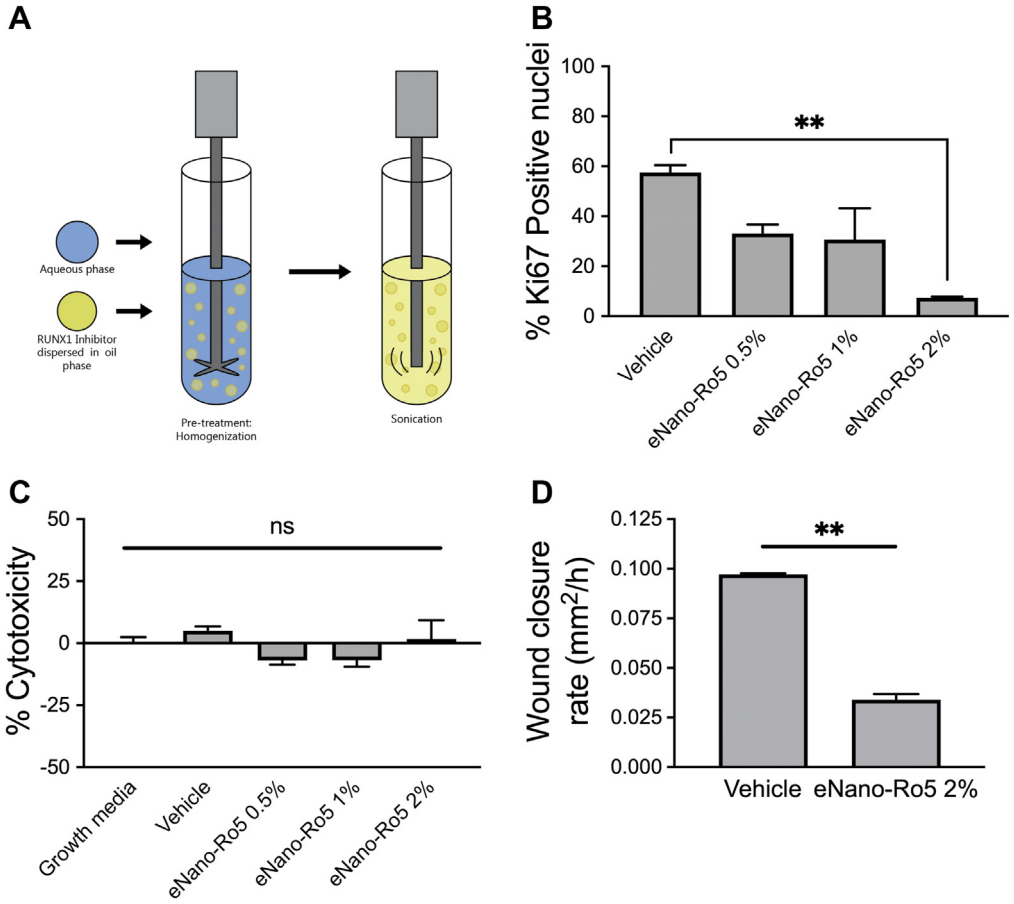

Figure 1. Modulation of runt-related transcription factor 1 (RUNX1) with eNano-Ro5 reduces migration and proliferation in endothelial cells. **A**, Schematic representation of the eNano-Ro5 manufacturing process. Oil and aqueous phase containing RUNX1 inhibitor are mixed by homogenization and sonication to generate a nanoemulsion. **B**, Bar graph showing the percentage of Ki67-positive nuclei relative to 4',6-diamidino-2-phenylindole (DAPI) after treatment with eNano-Ro5 effectively reduces the number of proliferating cells. Quantification of percentage of Ki67-positive cell nuclei shows a significant reduction in the group treated with eNano-Ro5 at 2% compared with the group treated with vehicle alone (Data are shown as mean ± standard error of the mean; 2-way analysis of variance; n = 4; experiments performed in triplicate; $^{**}P < 0.01$). **C**, Bar graph showing the low percentage of cell death that was obtained at every eNano-Ro5 concentration studied. **D**, Bar graph showing the scratch assay to evaluate migratory capacity of human retinal endothelial cells in vitro established that treatment with eNano-Ro5 significantly reduces migration of endothelial cells. (Data are shown as mean ± standard error of the mean; *t* test; n = 3; experiment performed in triplicate; $^{**}P < 0.01$.)

cornea. The rinsing procedure was performed with the mice in lateral recumbency and using absorbable pads with a water-based heating pad beneath the pads to keep the animals dry and to prevent inhalation of the water. Eyes were treated with antibiotic drops (Ofloxacin) 4 times daily for 3 days after the procedure. Then, on the fourth day after the procedure, a triple antibiotic ointment (Neomycin/Polymyxin B/Bacitracin) was used 4 times daily. Finally, a subcutaneous injection of buprenorphine (0.05−0.1 mg/kg; Buprenex [Reckitt Benckiser, Inc]) was performed in all animals after the procedure and was repeated every 8 to 12 hours for 72 hours for pain management.

Anterior Segment Evaluation. Clinical assessment of ocular surface was performed after alkali burn on days 1, 3, 7, and 14. Mice were manually restrained by the scruffing method, and anterior segment images were acquired using a digital camera (Nikon) attached to a slit lamp at ×16 magnification. Additionally, corneas were evaluated by sodium fluorescein staining (BioGlo; HUB Pharmaceuticals) and imaged with cobalt blue filter.

Laser-Induced Choroidal Neovascularization Model. Laser photocoagulation was performed as previously described.[14] In brief, using the Micron III image-guide system (Phoenix Research Labs) and a 532-nm laser (Merilas Laser), 4 laser spots were administered at the 3-, 6-, 9-, and 12-o'clock meridians at 2 to 3 disc diameters of distance from the optic nerve head. Applied laser parameters were 120 mW of power, 50 ms duration, and a spot size of 50 µm. Optimal alignment and focus of the eye with the camera were achieved for all procedures to induce consistent and reliable laser photocoagulation. Disruption of Bruch's membrane was confirmed by the appearance of a cavitation bubble at the site of the laser photocoagulation. Laser spots that did not result in the formation of a bubble were excluded from the study. Mice were euthanized and eyes were collected 7 days after laser induction.

Fluorescein Angiography. Fluorescein angiography was performed 6 days after laser induction, as described.[14] Under general anesthesia, 0.1 ml of 2% sodium fluorescein (Akorn) was administered intraperitoneally, and subsequent serial photographs from early phase (0−60 seconds after injection) and late phase (6 minutes after injection) were captured using the Micron III imaging system. Light source intensity and gain were standardized and maintained in all experiments.

Immunofluorescence. For corneal flat-mount preparation, eyes were fixed in 4% paraformaldehyde for 1 hour at 4°C. Corneas were dissected and blocked with 1% bovine serum albumin, 0.1% Triton X-100, and 3% donkey serum in Pblec buffer (0.1 mM CaCl2 , 0.1 mM MgCl2 , 0.1 mM MnCl2 in PBS) overnight at 4°C and were incubated with rat anti-CD31 (1:100; BD Biosciences) and rabbit anti-RUNX1 (1:100; LS-B13948 [Lifespan Biosciences]). Three washes with PBS were performed and secondary antibody donkey antirat Alexa Fluor 488 (1:300; Life Technologies) or donkey antirabbit Alexa Fluor 594 (1:300; Life Technologies) were incubated for 2 hours at room temperature in Pblec buffer. Then, samples were washed and mounted using Fluoromount-G (Thermo Fisher Scientific).

For choroidal flat-mount preparation, eyes were enucleated and submerged in 4% paraformaldehyde for 2 hours at 4°C for tissue fixation, as previously published.[14] After fixation, cornea, lens, and retina were removed, and 8 petals were created by cutting the remaining eye cup. Samples were blocked with 1% bovine serum albumin, 0.1% Triton X-100, and 3% donkey serum in Pblec buffer overnight at 4°C and were incubated with isolectin B4 (1:100; Alexa Fluor 488 Conjugate [Thermo Fisher Scientific]) and rabbit anti-RUNX1 (1:100; LS-B13948 [Lifespan Biosciences]) overnight at 4°C. Then, samples were washed 3 times with PBS and incubated with secondary antibody donkey antirabbit Alexa Fluor 594 (1:300; Life Technologies) for 2 hours at room temperature in Pblec buffer. Samples were washed again 3 times with PBS and then mounted with Fluoromount-G.

Immunostaining of Cryosections. Eyes were enucleated and fixed in 4% paraformaldehyde for 1 hour at room temperature for corneal cryosections and overnight at 4°C for retinal cryosections, then cryoprotected in increasing concentrations of sucrose before being embedded in OCT (Sakura Finetek) and frozen at −80°C. Sections 10-μm thick were obtained and then thawed, air dried, and incubated in blocking buffer containing 2% bovine serum albumin and 0.3% Triton X-100 for 30 minutes. Rat anti-CD31 (1:100; BD Biosciences), rabbit anti-RUNX1 (1:100; LS-B13948 [Lifespan Biosciences]), and conjugated rat anti-glial fibrillary acidic protein (GFAP) 594 (1:100; Agilent Dako) were used as primary antibodies. Donkey antirat Alexa Fluor 488 (1:300; Life Technologies) or donkey antirabbit Alexa Fluor 594 (1:300 [Life Technologies]) were incubated as secondary antibodies for 2 hours at room temperature and nuclei were stained with DAPI (Sigma Aldrich). For terminal deoxynucleotidyl transferase (TdT)-mediated uridine triphosphate (UTP) nick-end labeling assay, the In Situ Cell Death Detection Kit (Roche) was used following the manufacturer's instructions. All samples were imaged with an EVOS FL Auto imaging system. Confocal imaging was performed using the Leica SP8 confocal microscope (Leica).

Quantification of Corneal Neovascularization and Corneal Injury. Corneal neovascularization and corneal defect after alkali burn were measured using ImageJ (National Institutes of Health) at days 1, 3, 7, and 14 after model induction. A comprehensive analysis was carried out by multiple quantification analysis methods to obtain the most accurate results. Corneal defect area was measured by fluorescein staining. Each corneal epithelial defect area was quantified in pixels and then normalized to its total corneal area to avoid any variation in image acquisition. A corneal defect area to whole cornea ratio (%) was obtained as previously published.[20] Corneal neovascularization length was quantified by measuring the longest vessel from the limbus to the center of the cornea. Also, total neovascularization area was measured by obtaining a standardized representative corneal region of interest for each image to avoid variation, and then vessels were outlined using the Wand tool plug in (Versatile Wand Tool of ImageJ) in a semiquantitative manner. Finally, a qualitative score evaluating corneal opacity, corneal neovascularization, and corneal defect was performed in a randomized and masked fashion by 2 observers (S.D.-T., and L.G.-B.) based on previously published methodology.[21] Corneal opacity severity was graded as follows: 0 = completely clear; 1 = slightly hazy, iris and pupil easily visible; 2 = slightly opaque, iris and pupil still detectable; 3 = opaque, pupils hardly detectable; and 4 = completely opaque with no view of the pupil. Presence of corneal neovascularization was graded as follows: 0 = no neovessels, 1 = neovessels at the corneal limbus, 2 = neovessels spanning the corneal limbus and approaching the corneal center, and 3 = neovessels spanning the corneal center. Corneal defect severity scoring was as follows: 0 = no fluorescein staining, 1 = diffuse punctate keratitis, 2 = corneal ulcer, 3 = descemetocele, and 4 = corneal perforation.

Quantification of Choroidal Neovascularization Size and Vascular Leakage. Choroidal neovascularization (CNV) lesion size and vascular permeability were measured as previously described.[14] ImageJ software version 2.0.0 and the versatile Wand tool plug-in (Versatile Wand Tool of ImageJ) were used to delineate the neovascular complex and vascular leakage area in a semiquantitative manner. Lesion inclusion and exclusion criteria were established before quantification, as previously published.[22,23] All images were randomized, and were evaluated by 2 masked observers (L.G.-B., and M.A.) for analysis.

Mass Spectrometry in Mice Ocular Tissues for Detection of Ro5-3335. Eyes were collected after 24 and 72 hours of treatment and were dissected to obtain the cornea and posterior segment for separate analysis following a previously published method with slight modifications.[16] Each sample was subjected to solid−liquid extraction before liquid chromatography-tandem mass spectrometry analysis. In brief, cornea and posterior segment sections were sonicated (10 seconds at 0.5 kW) in 0.1 ml of tris buffered saline (pH, 7.4) 3 times onto ice with a Qsonica XL-2000 sonicator (Qsonica LLC). To allow mass transfer, an organic-phase n-butyl chloride 0.5 ml was added to each sample. Next, the samples were vortexed for 10 minutes and centrifuged at 10 000 rpm for 10 minutes. Following the collection of the supernatant, the procedure was repeated 3 times to ensure maximum extraction efficiency. Finally, the eluates were dried and reconstituted in 100 μl of dimethyl sulfoxide. To evaluate extraction efficiency of the method, samples were spiked with 30 ng/μl of Ro5-3335, and nonspiked tissues served as blanks. The recovery was analyzed by comparing the response of extracted and nonextracted samples (Fig 2D). Liquid chromatography-tandem mass spectrometry analysis technology was used to detect Ro5-3335 levels in each tissue. Calibration curves of Ro5 Ro5-3335 were prepared by serial dilutions in dimethyl sulfoxide to produce concentrations between 0.1 and 50 pg/μl. After solid−liquid extraction, liquid chromatography-tandem mass spectrometry analysis was performed as previously described.[16]

Statistical Analysis

Results are shown as mean ± standard error of the mean. A 2-tailed unpaired *t* test or 1-way or 2-way analysis of variance were used for statistical analysis with results as follows: NS = not significant, $*P < 0.05$, $**P \leq 0.01$, and $***P \leq 0.001$.

Results

In Vitro Effects of eNano-Ro5 in HRECs

We assessed the effect of a nanoemulsion containing Ro5-3335 in the proliferation and migration of HRECs,

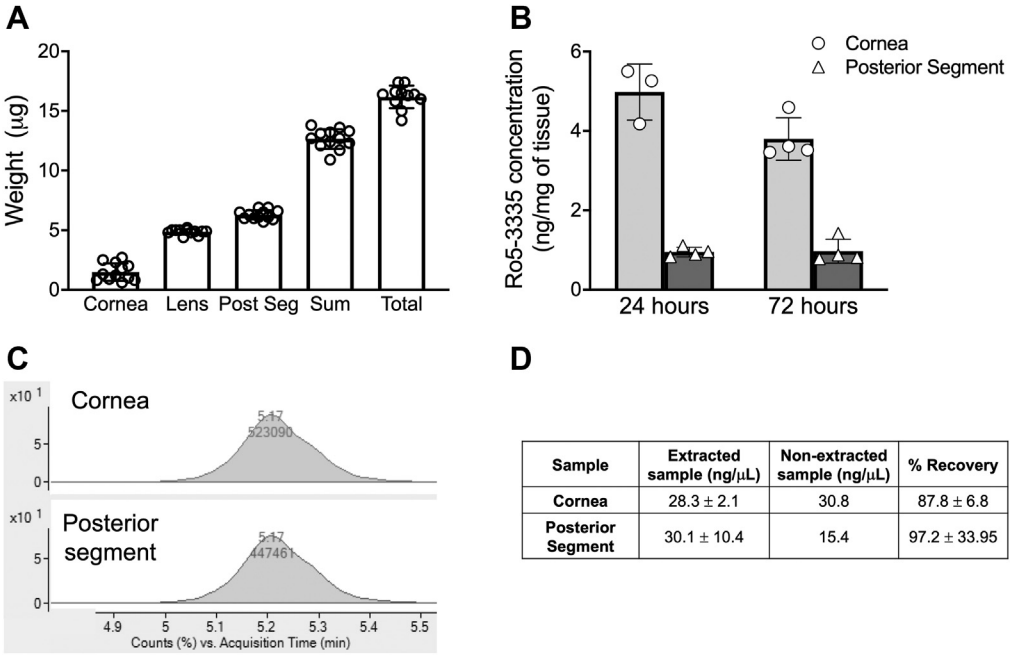

Sample	Extracted sample (ng/µL)	Non-extracted sample (ng/µL)	% Recovery
Cornea	28.3 ± 2.1	30.8	87.8 ± 6.8
Posterior Segment	30.1 ± 10.4	15.4	97.2 ± 33.95

Figure 2. Ocular pharmacokinetics of eNano-Ro5 in mice. **A**, Graph showing the determination of several ocular tissue weights in C57BL/6J mice. A detailed determination was performed to calculate liquid chromatography-tandem mass spectrometry results accurately. Data are shown as mean ± standard deviation (n = 12). **B**, Bar graph showing concentrations of small-molecule Ro5-3335 in the cornea and posterior segment in mice treated with topical nanoemulsion eNano-Ro5. Data are shown as mean ± standard deviation (n = 3 and n = 4). **C**, Quantitative liquid chromatography-tandem mass spectrometry analysis of Ro5-3335 in dimethyl sulfoxide. Typical chromatogram with a retention time of Ro5-3335 of 5.17 minutes. **D**, Table comparing nonextracted and extracted samples at a concentration of 50 µg/ml.

2 processes critical to angiogenesis. Ro5-3335 exposure induced a dose-dependent reduction of Ki67-positive nuclei, a marker of proliferation, reaching a statistically significant reduction of 86% with the 2% eNano-Ro5 concentration (Fig 1B). Interestingly, no significant cell death percentage was observed at any of the tested concentrations (Fig 1C). In addition, the 2% eNano-Ro5 concentration significantly reduced HREC migration by 65% (Fig 1D).

Ro5-3335 Is Detectable in Mouse Ocular Tissues after Topical Application

We performed liquid chromatography-tandem mass spectrometry to investigate whether eNano-Ro5 was delivering Ro5-3335 effectively to ocular tissues. Each mouse tissue was independently weighed for normalization and posterior liquid chromatography-tandem mass spectrometry analysis (Fig 2A). Mice were treated with 1 drop of topical eNano-Ro5 4 times daily for 24 and 72 hours. Mice were manually restrained by the scruffing method for 60 seconds to ensure correct application and absorption of topical treatment. We removed nanoemulsion excess using a cotton spear to avoid any oral absorption of the drug as a result of licking and grooming after the treatment. We detected Ro5-3335 in the cornea and the posterior segment of the mice, proving effective delivery of eNano-Ro5 in mice. We found Ro5-3335 in the cornea with a concentration of 4.98 ng/mg and 3.79 ng/mg at 24 and 72 hours, respectively. Also, detectable levels were observed in the posterior segment samples of 0.95 ng/mg and 0.97 ng/mg at each time point (Fig 2B). Ro5-3335 retention time was observed at 5.17 minutes (Fig 2C). High levels of percentage recovery suggest a highly efficient solid−liquid extraction process (Fig 2D). Significant delivery to the retina was also confirmed in a published rabbit model of proliferative vitreoretinopathy.[16]

eNano-Ro5 Induces Faster Recovery and Curbs Neovessel Formation after Alkali Burn-Induced Corneal Neovascularization

We detected RUNX1-positive cells within corneal tissue 14 days after corneal alkali burn. A small population of the RUNX1-positive cells observed in the injured cornea showed costaining with CD31, identifying them as vascular endothelial cells (Fig 3A, B). We treated mice 4 times daily for 14 days with eNano-Ro5 (7.92 mM) or vehicle after alkali burn injury to evaluate therapeutic response (Fig 3C, D). Corneal opacity was significantly improved at days 1, 7, and 14 in the eyes treated with eNano-Ro5 compared with those treated with vehicle alone (Fig 3D). Because of decreased corneal opacification, ocular media are more transparent and a cataractous lens is visible. eNano-Ro5 treatment reduced corneal neovascularization after 14 days of topical treatment as measured by 3 different quantification methods, including neovascularization length, neovascularization area, and neovascularization score (Fig 3E−G). At day 14, the corneal defect score was significantly improved in the

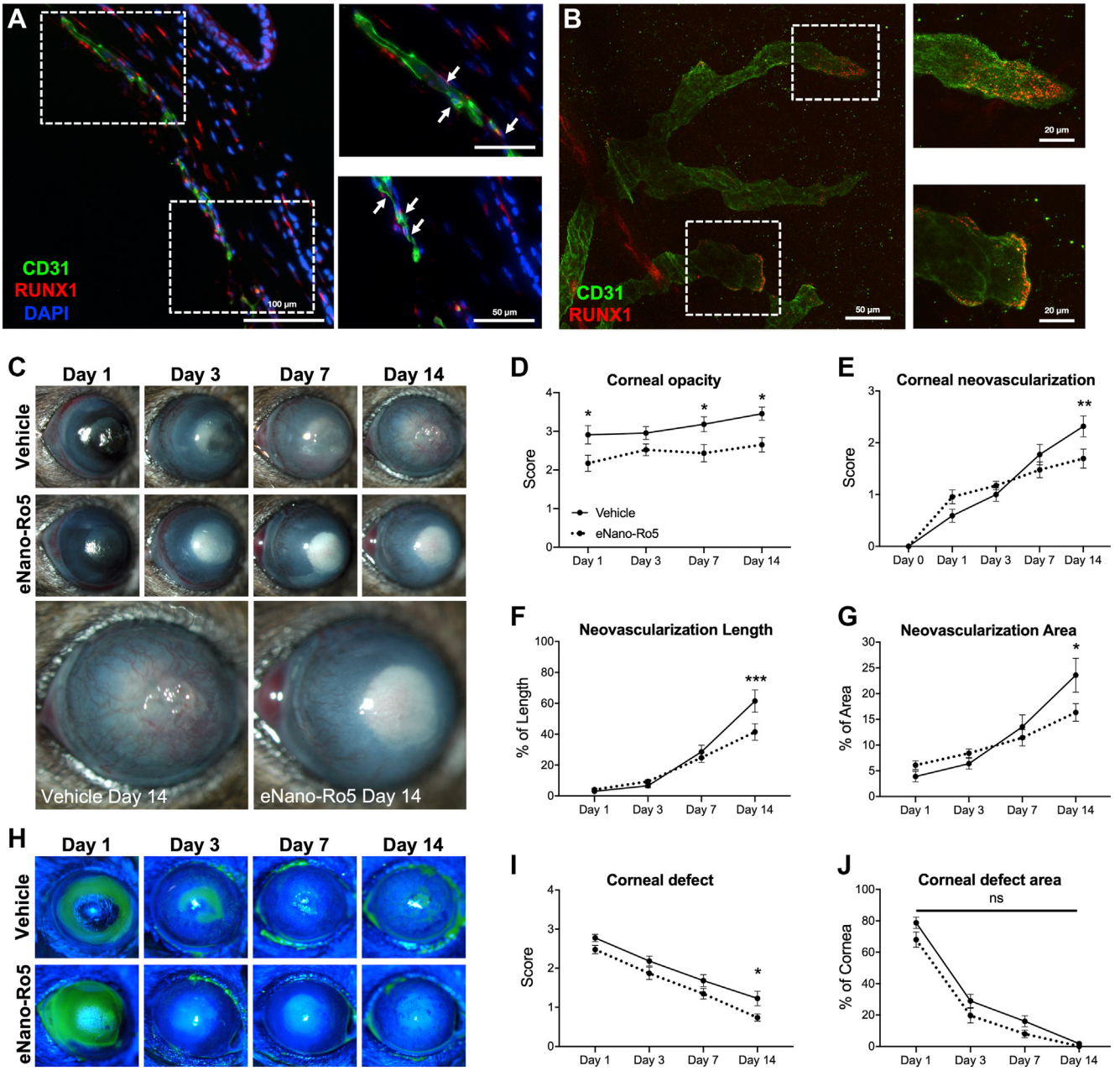

Figure 3. Treatment with eNano-Ro5 improves outcomes in an alkali-burn neovascularization model. **A**, Immunofluorescence of corneal sections showing the presence costaining of runt-related transcription factor 1 (RUNX1)-positive cells and the endothelial cell marker CD31 (arrows). Scale bar (top) = 100 μm. Dotted squares represent magnified areas. Scale bar (bottom) = 50 μm. **B**, Confocal imaging showing colocalization of RUNX1 and CD31 in corneal neovessels. Scale bar (top) = 50 μm. Dotted squares represent magnified areas. Scale bar (bottom) = 20 μm. **C**, Representative images of mice treated with either vehicle or eNano-Ro5 on days 1, 3, 7, and 14 after treatment. **D**–**G**, Graphs showing that topical treatment of eNano-Ro5 successfully improved corneal opacity and reduced neovascularization at different time points. (Data are shown as mean ± standard error of the mean; vehicle, n = 22 mice; eNano-Ro5, n = 23 mice; 2-way analysis of variance; *$P < 0.05$; **$P < 0.01$; ***$P < 0.001$.) **H**, Sodium fluorescein staining showing corneal ulcer healing over time. **I, J**, Graphs showing that topical treatment with RUNX1 small-molecule inhibitor Ro5-3335 improved corneal re-epithelization. DAPI = 4',6-diamidino-2-phenylindole.

group treated with eNano-Ro5 compared with control (Fig 3I); however, no significant differences were observed in the corneal defect area (Fig 3J).

Additionally, we included another group treated with topical steroids 4 times daily using dexamethasone sodium phosphate ophthalmic solution, United States Pharmacopeia 0.1% (Bausch & Lomb). After 14 days of treatment, we observed significantly reduced corneal opacity and less neovascularization compared with vehicle. However, the corneal defect area and epithelial defect score were significantly increased as a result of wound-healing process impairment. When comparing eNano-Ro5 and dexamethasone, both

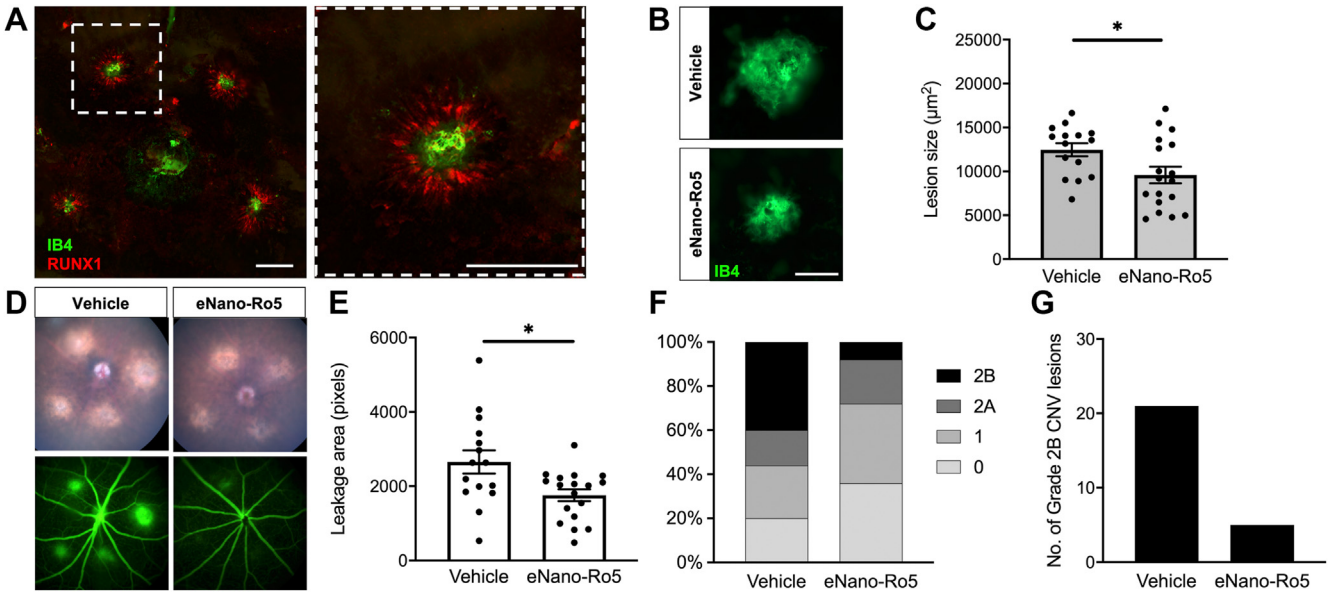

Figure 4. Effects of topical treatment with nanoemulsion containing small-molecule runt-related transcription factor 1 (RUNX1) inhibitor in a laser-induced choroidal neovascularization (CNV) model. **A**, Choroidal flat-mount stained with isolectin B4 (green) labeling neovascular complex and RUNX1 (red) 7 days after laser induction. Note the high expression levels of RUNX1 in injured areas, but not in surrounding tissues. Dotted square depicts magnified areas. Scale bars = 200 µm. **B**, Representative images of CNV stained with isolectin B4 in both treated groups. Scale bar = 100 µm. **C**, Quantification of lesion size showing that topical treatment with eNano-Ro5 reduces neovascular complex size. (Data are shown as mean ± standard error of the mean; vehicle, n = 15; eNano-Ro5, n = 18; *t* test; **P* <0.05.) **D**, Representative images of funduscopy (top) and fluorescein angiography (bottom) 6 days after laser in the mice treated with vehicle (left) or eNano-Ro5 (right). **E**, Quantification of CNV leakage demonstrating that topical treatment with RUNX1 inhibitor significantly curbed vascular leakage from CNV lesions. (Data are shown as mean ± standard error of the mean; vehicle, n = 15; eNano-Ro5, n = 18; *t* test; **P* <0.05.) **F**, Leakage severity grading showing less severe lesions in the mice treated with eNano-Ro5 compared with those treated with vehicle. **G**, Bar graph showing total number of grade 2B lesions in both study groups.

treatments significantly reduced corneal neovascularization and improved corneal opacity compared with vehicle, with dexamethasone slightly superior to eNano-Ro5. However, as mentioned earlier, corneal epithelial defect resolution was significantly reduced by dexamethasone, whereas eNano-Ro5 improved wound healing at day 14. Importantly, we lost some of the eyes treated with steroids because of corneal perforation precipitated by corneal melting and delayed wound-healing response (Supplemental Fig S1).

Topical Application of eNano-Ro5 Reduces CNV Lesion Size and Vascular Permeability

We measured neovascular complex size and severity of vascular leakage after treatment with either topical eNano-Ro5 (7.92 mM) or vehicle 4 times daily over 7 days. We measured CNV lesion area in choroidal flat-mount preparations stained with isolectin B4 to measure neovascularization (Fig 4A, B). We observed a significant reduction of 23% in CNV lesion area in the group treated with eNano-Ro5 (9588.12 ± 939.2 µm^2) when compared with vehicle (12 465 ± 739.2 µm^2) after treatment (Fig 4C). To rule out any effect of the vehicle in the therapeutic response, a third group was included in which laser injury was performed, but no treatment was applied. No significant differences between the untreated group (15 095 ± 2259 µm^2) and the vehicle-treated group (12 465 ± 739.2 µm^2) were observed (Supplemental Fig S2). To see additional extended treatment duration (14 days), see Supplemental Figure S3.

We also evaluated therapeutic response by grading the level of leakage obtained in fluorescein angiograms (Fig 4D). Vascular permeability was reduced by 34% in mice treated with eNano-Ro5 (1758 ± 159.6 pixels) compared with those treated with vehicle (2655 ± 312.8 pixels; Fig 4E). We observed robust differences in the distribution of the severity of lesions between the eNano-Ro5–treated mice compared with the control group (Fig 4F). Specifically, the total number of grade 2B lesions was dramatically reduced in the mice treated with eNano-Ro5 (Fig 4G). No significant differences in vascular leakage were observed comparing untreated mice and those treated with vehicle (Supplemental Fig S2).

Topical application of nanoemulsion containing RUNX1 inhibitor seems to be safe and well tolerated. No significant differences were obtained in TdT-mediated UTP nick-end labeling–positive cells or Glial Fibrillary Acidic Protein expression after topical application of eNano-Ro5 for 7 days in both corneal and retinal sections (Supplemental Fig S4). Electroretinograms showing no differences between mice treated with eNano-Ro5 and control mice were recently published.[16]

Discussion

Aberrant ocular neovascularization is a pathophysiologic process that contributes to multiple blinding diseases affecting both the anterior and the posterior segments of the

eye. Currently, no effective treatment exists for the neovascularization of the anterior segment of the eye that primarily affects the cornea. Neovascularization affecting the posterior segment of the eye, including retinal and choroidal angiogenesis, is treated effectively with anti-VEGF therapies. However, current anti-VEGF drugs are biologics requiring repeated intravitreal injections that are onerous to the patient, require specialized personnel for administration, carry the risk of endophthalmitis, are incompatible with social distancing protocols, and add significant financial burden to the health care system. Thus, a need exists to investigate and develop alternate therapies to improve the management of these conditions. Herein, we investigated the effect of an eNano-Ro5 nanoemulsion topically administered in experimental corneal and choroidal neovascularization.

The role of RUNX1 in aberrant angiogenesis has been reported in various animal models by our group.[13,14] Runt-related transcription factor 1 inhibition by small interfering RNA and small molecules significantly reduced all hallmarks of angiogenesis in vascular endothelial cells in culture, including migration, proliferation, and tube formation.[13] Herein, we showed that delivering an RUNX1 inhibitor from a nanoemulsion formulation results in similar effects of curbing the hallmarks of angiogenesis in vitro. This observation confirms the role of RUNX1 in endothelial cell homeostasis and demonstrates that the nanoemulsion is able to successfully release the drug, reaching effective concentrations to modulate endothelial cell function in vitro. A detailed characterization and release profile of Ro5-3335 from eNano-Ro5 was recently published.[16]

Over the last 2 decades, new platforms have been developed to deliver drugs effectively to ocular tissues, while maintaining effective drug concentrations.[24] Topical eye drops remain the most common method of treatment for ocular diseases (i.e., open-angle glaucoma and postoperative inflammation, among others).[25,26] Although there are no clear guidelines for the management of corneal angiogenesis, a wide range of options to treat these abnormal blood vessels exist, including both medical (topical steroids, topical nonsteroidal anti-inflammatory agents, anti-VEGF drugs, etc.) and surgical (amniotic membrane transplantation, ocular surface stem cell transplantation, fine-needle diathermy, etc.) treatments, yet each comes with limited efficacy and considerable side effects.[2,27,28]

Drug delivery to effectively treat posterior segment diseases in humans is challenging and has been investigated for many years. However, the treatment of posterior segment diseases is restricted by physical and physiologic obstacles that prevent many drugs from reaching therapeutic concentrations. This limits the efficacy of this route of administration and makes intravitreal injections the method of choice to treat these diseases.[29,30] Many studies investigating the use of topical eyedrops to treat retinal diseases, such as AMD or diabetic retinopathy, have been unsuccessful,[31–33] whereas other topical eye drops are commonly used and are effective in daily clinical practice (i.e., steroids or nonsteroidal anti-inflammatory drugs for cystoid macular edema).[26,34] This precedent of failure in part could be because most drugs previously tested included kinase inhibitors that have short duration of signaling effects, or antibodies with limited penetration through ocular barriers because of their molecular weight.[31–33] Herein, we used Ro5-3335, a small, highly lipophilic molecule targeting a transcription factor expected to have a long duration of downstream effects. We surmise that topical administration of a RUNX1 inhibitor with a high concentration of active ingredient encapsulated in the nanoemulsion and repeated doses for a long duration of treatment may result in effective therapy. High concentration of active drug and repeated dosing have been reported to be critical to increase corneal permeability to optimize drug delivery in the posterior structures in the back of the eye.[24,35,36] One study used a similar approach by encapsulating bevacizumab in topical liposomal carrier and reached remarkable levels of bevacizumab in vivo.[37] However, no results have been published yet in animal models using this carrier.

Treatment with eNano-Ro5 after alkali burn achieved a significant reduction of corneal opacity and neovascularization and a faster recovery of corneal defect. Corneal opacity in the early time points is mainly the result of corneal edema and inflammation, whereas in the late time points, it is likely the result of corneal fibrosis. However, further studies are needed to confirm changes in EMT markers in the cornea, in addition to evaluating the effect of RUNX1 in the inflammatory cascade. We observed a reduction in corneal opacity at all the time points studied, suggesting that eNano-Ro5 may decrease the inflammatory response after alkali burn and the development of fibrosis. Previous reports have highlighted the role of RUNX1 in inflammation and wound-healing response processes.[15,16,38] Further investigation is needed in this regard to evaluate the effect of RUNX1 in the inflammatory cascade. Topical steroids treatment was superior to eNano-Ro5 in reducing corneal opacity. We believe that because of decreased corneal wound healing and decreased corneal defect resolution, corneal transparency was maintained. Although corneal neovascularization was significantly reduced with both treatments, dexamethasone was slightly superior than eNano-Ro5 at some time points.

Corneal defect, along with corneal neovascularization, is also present in multiple eye diseases and potentially can threaten the integrity of the eye if complicated with infection or perforation. We observed a faster resolution of the corneal defect after alkali burn in the group treated with eNano-Ro5. Topical steroids are widely used for the treatment of many corneal conditions, but as demonstrated in this study, the delay of the resolution of corneal ulcers has been associated with these drugs, limiting their use in certain situations.[39,40] Surprisingly, treatment with Ro5-3335 promoted a faster resolution of the corneal defect, which warrants further investigation. Treatment with eNano-Ro5 seems to reach a balance in terms of safety and efficacy, combining the benefits of steroid therapy (improved corneal opacity and reduced neovascularization) without its drawbacks (faster resolution of corneal defect and no corneal perforation).

With regard to choroidal neovascularization, treatment with eNano-Ro5 significantly reduced lesion size and vascular leakage in a laser-induced CNV model. Our group recently published similar results with intravitreal injection of Ro5-3335,[14] but the present study also proves the efficacy of this drug via topical administration, which, if validated in clinical trials, could be potentially transformative for the management of prevalent diseases such as neovascular AMD. Also, importantly, our previous report using intravitreal injection of Ro5-3335 alone did not show significant reduction of leakage when used in monotherapy, whereas topical eNano-Ro5 treatment was effective. This may suggest that topical administration may be a more effective method of drug delivery for a small-molecule RUNX1 inhibitor.

Our data show promising results of RUNX1 inhibition by topical administration of eNano-Ro5 in experimental ocular neovascularization. Additionally, topical RUNX1 inhibition has been shown to reduce inflammation and EMT,[16,38] which leads to fibrosis and irreversible vision loss in multiple eye conditions. Deeper understanding of the role of RUNX1 in ocular diseases may help us to develop new therapeutic strategies to control the devastating effects of aberrant angiogenesis, inflammation, and fibrosis in various eye diseases.

Footnotes and Disclosures

Originally received: October 11, 2021.
Final revision: April 5, 2022.
Accepted: April 14, 2022.
Available online: April 20, 2022. Manuscript no. XOPS-D-21-00187.

[1] Schepens Eye Research Institute, Massachusetts Eye and Ear, Boston, Massachusetts.

[2] Department of Ophthalmology, Harvard Medical School, Boston, Massachusetts.

[3] Department of Ophthalmology, Puerta de Hierro-Majadahonda University Hospital, Madrid, and Department of Ophthalmology, Castilla La Mancha University, Albacete, Spain.

[4] Energy, Materials and Environment Group, Faculty of Engineering, Universidad de La Sabana, Chia, Colombia.

[5] Department of Biomedical Engineering and Chemical Engineering, University of Texas at San Antonio, San Antonio, Texas.

[6] Instituto de Microcirugía Ocular (IMO), Madrid, and VISSUM, Alicante, Spain.

[7] Universidad EIA, Envigado, Antioquia, Colombia.

Presented at: Association for Research in Vision and Ophthalmology (ARVO) Annual Meeting, May, 2019, Vancouver, BC, Canada; Presented as a poster at: Association for Research in Vision and Ophthalmology (ARVO) Annual Meeting, May, 2021, Virtual.

*Both authors contributed equally as first authors.

Disclosure(s):

All authors have completed and submitted the ICMJE disclosures form.

The author(s) have made the following disclosure(s): J.F.A.-V.: Patent — W02019099595 (Nano-emulsion of CBFβ-RUNX1 Inhibitor for Ocular Drug Delivery) 11229662 (Composition and Methods for the Treatment of Aberrant Angiogenesis)

L.A.K.: Patent — W02019099595 (Nano-emulsion of CBFβ-RUNX1 Inhibitor for Ocular Drug Delivery) 11229662 (Composition and Methods for the Treatment of Aberrant Angiogenesis)

Supported by the National Institute of Neurological Disorders and Stroke and the National Institute on Aging (grant nos.: NS100121, NS110048, and 1U01NS119560) and the National Eye Institute (grant nos.: R01 EY027739 and P30 EY003790), National Institutes of Health, Bethesda, Maryland; the E. Matilda Ziegler Foundation for the Blind; the Karl Kirchgessner Foundation; the Alfonso Martin Escudero Foundation, Spain; COLCIENCIAS doctoral training scholarship (award no. 727-2015), Colombia; and Michel Plantevin funds. The sponsor or funding organization had no role in the design or conduct of this research.

HUMAN SUBJECTS: No human subjects were included in this study.

Nonhuman animals were used in a study. Protocol was approved by Institutional Animal Care and Use Committee of Massachusetts Eye and Ear. All experiments were done in accordance with the Association for Research in Vision and Ophthalmology Statement for the Use of Animals in Ophthalmic and Vision Research.

Author Contributions:

Conception and design: Delgado-Tirado, Gonzalez-Buendia, Arboleda-Velasquez, Kim

Analysis and interpretation: Delgado-Tirado, Gonzalez-Buendia, Ruiz-Moreno, Arboleda-Velasquez, Kim

Data collection: Delgado-Tirado, Gonzalez-Buendia, An, Amarnani, Isaacs-Bernal, Whitmore, Arevalo-Alquichire, Leyton-Cifuentes

Obtained funding: N/A

Overall responsibility: Delgado-Tirado, Gonzalez-Buendia, Ruiz-Moreno, Arboleda-Velasquez, Kim

Abbreviations and Acronyms:
AMD = age-related macular degeneration; **CNV** = choroidal neovascularization; **EMT** = epithelial-to-mesenchymal transition; **HREC** = human retinal endothelial cell; **PBS** = phosphate-buffered saline; **RUNX1** = runt-related transcription factor 1.

Keywords:
Choroidal neovascularization, Cornea neovascularization, RUNX1, Topical ophthalmic, Treatment.

Correspondence:
Leo A. Kim, MD, PhD, Schepens Eye Research Institute, 20 Staniford Street, Boston, MA 02114. E-mail: Leo_Kim@meei.harvard.edu; and Joseph F. Arboleda-Velasquez, MD, PhD, Schepens Eye Research Institute, 20 Staniford Street, Boston, MA 02114. E-mail: joseph_arboleda@meei.harvard.edu.

References

1. Kim LA, D'Amore PA. A brief history of anti-VEGF for the treatment of ocular angiogenesis. *Am J Pathol*. 2012;181(2):376–379.

2. Roshandel D, Eslani M, Baradaran-Rafii A, et al. Current and emerging therapies for corneal neovascularization. *Ocul Surf*. 2018;16(4):398–414.

3. Ferrara N. VEGF and intraocular neovascularization: from discovery to therapy. *Transl Vis Sci Technol*. 2016;5(2):10.
4. Rosenfeld PJ, Brown DM, Heier JS, et al. Ranibizumab for neovascular age-related macular degeneration. *N Engl J Med*. 2006;355(14):1419–1431.
5. Martin DF, Maguire MG, Ying GS, et al. Ranibizumab and bevacizumab for neovascular age-related macular degeneration. *N Engl J Med*. 2011;364(20):1897–1908.
6. Hsu YJ, Hsieh YT, Yeh PT, et al. Combined tractional and rhegmatogenous retinal detachment in proliferative diabetic retinopathy in the anti-VEGF era. *J Ophthalmol*. 2014;2014:917375.
7. Hsu J, Khan MA, Shieh WS, et al. Effect of serial intrasilicone oil bevacizumab injections in eyes with recurrent proliferative vitreoretinopathy retinal detachment. *Am J Ophthalmol*. 2016;161:65–70.
8. Saint-Geniez M, Maharaj AS, Walshe TE, et al. Endogenous VEGF is required for visual function: evidence for a survival role on Müller cells and photoreceptors. *PloS One*. 2008;3(11):e3554.
9. Sang DN, D'Amore PA. Is blockade of vascular endothelial growth factor beneficial for all types of diabetic retinopathy? *Diabetologia*. 2008;51(9):1570–1573.
10. Bhisitkul RB, Mendes TS, Rofagha S, et al. Macular atrophy progression and 7-year vision outcomes in subjects from the ANCHOR, MARINA, and HORIZON studies: the SEVEN-UP study. *Am J Ophthalmol*. 2015;159(5):915–924.e2.
11. Mettu PS, Allingham MJ, Cousins SW. Incomplete response to Anti-VEGF therapy in neovascular AMD: exploring disease mechanisms and therapeutic opportunities. *Prog Retin Eye Res*. 2021;82:100906.
12. Lee P, Wang CC, Adamis AP. Ocular neovascularization: an epidemiologic review. *Surv Ophthalmol*. 1998;43(3):245–269.
13. Lam JD, Oh DJ, Wong LL, et al. Identification of RUNX1 as a mediator of aberrant retinal angiogenesis. *Diabetes*. 2017;66(7):1950–1956.
14. Gonzalez-Buendia L, Delgado-Tirado S, An M, et al. Treatment of experimental choroidal neovascularization via RUNX1 inhibition. *Am J Pathol*. 2021;191(3):418–424.
15. Whitmore HAB, Amarnani D, O'Hare M, et al. TNF-α signaling regulates RUNX1 function in endothelial cells. *Faseb J*. 2021;35(2):e21155.
16. Delgado-Tirado S, Amarnani D, Zhao G, et al. Topical delivery of a small molecule RUNX1 transcription factor inhibitor for the treatment of proliferative vitreoretinopathy. *Sci Rep*. 2020;10(1):20554.
17. Kuiper EJ, Van Nieuwenhoven FA, de Smet MD, et al. The angio-fibrotic switch of VEGF and CTGF in proliferative diabetic retinopathy. *PloS One*. 2008;3(7):e2675.
18. Liang CC, Park AY, Guan JL. In vitro scratch assay: a convenient and inexpensive method for analysis of cell migration in vitro. *Nat Protoc*. 2007;2(2):329–333.
19. Kilkenny C, Browne WJ, Cuthill IC, et al. Improving bioscience research reporting: the ARRIVE guidelines for reporting animal research. *PLoS Biol*. 2010;8(6):e1000412.
20. Zhou C, Robert MC, Kapoulea V, et al. Sustained subconjunctival delivery of infliximab protects the cornea and retina following alkali burn to the eye. *Invest Ophthalmol Vis Sci*. 2017;58(1):96–105.
21. Anderson C, Zhou Q, Wang S. An alkali-burn injury model of corneal neovascularization in the mouse. *J Vis Exp*. 2014;86:51159.
22. Poor SH, Qiu Y, Fassbender ES, et al. Reliability of the mouse model of choroidal neovascularization induced by laser photocoagulation. *Invest Ophthalmol Vis Sci*. 2014;55(10):6525–6534.
23. Gong Y, Li J, Sun Y, et al. Optimization of an image-guided laser-induced choroidal neovascularization model in mice. *PloS One*. 2015;10(7):e0132643.
24. Del Amo EM, Rimpela AK, Heikkinen E, et al. Pharmacokinetic aspects of retinal drug delivery. *Prog Retin Eye Res*. 2017;57:134–185.
25. Geroski DH, Edelhauser HF. Drug delivery for posterior segment eye disease. *Invest Ophthalmol Vis Sci*. 2000;41(5):961–964.
26. Russo A, Costagliola C, Delcassi L, et al. Topical nonsteroidal anti-inflammatory drugs for macular edema. *Mediators Inflamm*. 2013;2013:476525.
27. Gupta D, Illingworth C. Treatments for corneal neovascularization: a review. *Cornea*. 2011;30(8):927–938.
28. Feizi S, Azari AA, Safapour S. Therapeutic approaches for corneal neovascularization. *Eye Vis (Lond)*. 2017;4:28.
29. Koevary SB, Nussey J, Lake S. Accumulation of topically applied porcine insulin in the retina and optic nerve in normal and diabetic rats. *Invest Ophthalmol Vis Sci*. 2002;43(3):797–804.
30. Takahashi K, Saishin Y, Saishin Y, et al. Topical nepafenac inhibits ocular neovascularization. *Invest Ophthalmol Vis Sci*. 2003;44(1):409–415.
31. Hu S, Koevary S. Efficacy of antibody delivery to the retina and optic nerve by topical administration. *J Ocul Pharmacol*. 2016;32(4):203–210.
32. Joussen AM, Wolf S, Kaiser PK, et al. The Developing Regorafenib Eye Drops for Neovascular Age-Related Macular Degeneration (DREAM) study: an open-label phase II trial. *Br J Clin Pharmacol*. 2019;85(2):347–355.
33. Csaky KG, Dugel PU, Pierce AJ, et al. Clinical evaluation of pazopanib eye drops versus ranibizumab intravitreal injections in subjects with neovascular age-related macular degeneration. *Ophthalmology*. 2015;122(3):579–588.
34. Asahi MG, Bobarnac Dogaru GL, et al. Strong topical steroid, NSAID, and carbonic anhydrase inhibitor cocktail for treatment of cystoid macular edema. *Int Med Case Rep J*. 2015;8:305–312.
35. Kidron H, Vellonen KS, del Amo EM, et al. Prediction of the corneal permeability of drug-like compounds. *Pharm Res*. 2010;27(7):1398–1407.
36. Worth AP, Cronin MT. Structure-permeability relationships for transcorneal penetration. *Altern Lab Anim*. 2000;28(3):403–413.
37. Davis BM, Normando EM, Guo L, et al. Topical delivery of Avastin to the posterior segment of the eye in vivo using annexin A5-associated liposomes. *Small*. 2014;10(8):1575–1584.
38. O'Hare M, Amarnani D, Whitmore HAB, et al. Targeting runt-related transcription factor 1 prevents pulmonary fibrosis and reduces expression of severe acute respiratory syndrome coronavirus 2 host mediators. *Am J Pathol*. 2021;191(7):1193–1208.
39. Hossain P. The corneal melting point. *Eye (Lond)*. 2012;26(8):1029–1030.
40. Barba KR, Samy A, Lai C, et al. Effect of topical anti-inflammatory drugs on corneal and limbal wound healing. *J Cataract Refract Surg*. 2000;26(6):893–897.